

**A cross-validation of FDG- and amyloid-PET biomarkers in MCI for the risk prediction to dementia due to Alzheimer's Disease in a clinical setting**

Leonardo Iaccarino<sup>a,b</sup>, Konstantinos Chiotis<sup>c</sup>, Pierpaolo Alongi<sup>d,e</sup>, Ove Almkvist<sup>c,f,g</sup>, Anders Wall<sup>h,i</sup>, Chiara Cerami<sup>b,j</sup>, Valentino Bettinardi<sup>d</sup>, Luigi Gianolli<sup>d</sup>, Agneta Nordberg<sup>c,g</sup> and Daniela Perani<sup>a,b,d\*</sup>

<sup>a</sup> Vita-Salute San Raffaele University, Milan, Italy

<sup>b</sup> In Vivo Human Molecular and Structural Neuroimaging Unit, Division of Neuroscience, IRCCS San Raffaele Scientific Institute, Milan, Italy

<sup>c</sup> Dept NVS, Center for Alzheimer Research, Translational Alzheimer Neurobiology, Karolinska Institutet, Stockholm, Sweden

<sup>d</sup> Nuclear Medicine Unit, IRCCS San Raffaele Hospital, Milan, Italy

<sup>e</sup> Department of Radiological Sciences, Nuclear Medicine Unit, San Raffaele G.Giglio Institute, Cefalù, Italy

<sup>f</sup> Department of Psychology, Stockholm University, Stockholm, Sweden

<sup>g</sup> Department of Geriatric Medicine, Karolinska University Hospital Huddinge, Stockholm, Sweden

<sup>h</sup> Radiology, Department of Surgical Sciences, Uppsala University, Uppsala, Sweden

<sup>i</sup> PET Centre, Uppsala University Hospital, Uppsala, Sweden

<sup>j</sup> Neurological Rehabilitation Unit, Department of Clinical Neurosciences, IRCCS San Raffaele Hospital, Milan, Italy

**Please address correspondence to:**

Prof. Daniela Perani

Vita-Salute San Raffaele University

Division of Neuroscience, IRCCS San Raffaele Scientific Institute

Nuclear Medicine Unit, IRCCS San Raffaele Hospital

Via Olgettina 60, 20132, Milan, Italy

e-mail:perani.daniela@hsr.it ; Tel. (+39)02.2643.2224; Fax: (+39)02.2643.2717

**Short Title:** FDG- and Amy-PET in MCI conversion prediction

**Reference:** Iaccarino, L., Chiotis, K., Alongi, P., Almkvist, O., Wall, A., Cerami, C., Bettinardi, V., Gianolli, L., Nordberg, A. and Perani, D. A Cross-Validation of FDG-and Amyloid-PET Biomarkers in Mild Cognitive Impairment for the Risk Prediction to Dementia due to Alzheimer's Disease in a Clinical Setting (2017). *Journal of Alzheimer's Disease*. 59(2), 603–614. <http://doi.org/10.3233/JAD-170158>

**URL:** <https://content.iospress.com/articles/journal-of-alzheimers-disease/jad170158>

## Abstract

Assessments of brain glucose metabolism ( $^{18}\text{F}$ -FDG-PET) and cerebral amyloid burden ( $^{11}\text{C}$ -PiB-PET) in Mild Cognitive Impairment (MCI) have shown highly variable performances when adopted to predict progression to dementia due to Alzheimer's Disease (ADD). This study investigates, in a clinical setting, the separate and combined values of  $^{18}\text{F}$ -FDG-PET and  $^{11}\text{C}$ -PiB-PET in ADD conversion prediction with optimized data analysis procedures. Respectively, we investigate the accuracy of an optimized SPM analysis for  $^{18}\text{F}$ -FDG-PET and of Standardized Uptake Value Ratio (SUVR) semiquantification for  $^{11}\text{C}$ -PiB-PET in predicting ADD conversion in 30 MCI subjects (age  $63.57 \pm 7.78$  years). Fourteen subjects converted to ADD during the follow-up (median 26.5 months, inter-quartile range 30 months). Receiver Operating Characteristic analyses showed an Area Under the Curve (AUC) of 0.89 and of 0.81 for, respectively,  $^{18}\text{F}$ -FDG-PET and  $^{11}\text{C}$ -PiB-PET.  $^{18}\text{F}$ -FDG-PET, compared to  $^{11}\text{C}$ -PiB-PET, showed higher specificity (1.00 vs. 0.62, respectively), but lower sensitivity (0.79 vs. 1.00). Combining the biomarkers improved classification accuracy (AUC=0.96). During the follow-up time, all the MCI subjects positive for both PET biomarkers converted to ADD, whereas all the subjects negative for both remained stable. The difference in survival distributions was confirmed by a log-rank test ( $p=0.002$ ). These results indicate a very high accuracy in predicting MCI to ADD conversion of both  $^{18}\text{F}$ -FDG-PET and  $^{11}\text{C}$ -PiB-PET imaging, the former showing optimal performance based on the SPM optimized parametric assessment. Measures of brain glucose metabolism and amyloid load represent extremely powerful diagnostic and prognostic biomarkers with complementary roles in prodromal dementia phase, particularly when tailored to individual cases in clinical settings.

**Keywords:** Mild Cognitive Impairment; Alzheimer Disease;  $^{18}\text{F}$ -FDG-PET;  $^{11}\text{C}$ -PiB-PET; Dementia conversion prediction; Prognosis; Early diagnosis

## 1. Introduction

The Mild Cognitive Impairment (MCI) construct is nowadays the most clinically valid entity to define a stage of possible transition from moderate cognitive impairment in aging to dementia. However, the trajectories of cognitive decline and the conversion to different forms of dementia call for the identification of optimal biomarkers for outcome prediction [1]. The risk prediction of conversion to dementia due to Alzheimer's Disease (ADD) has crucial implications for the best fitting in clinical trials of subjects with correct AD diagnosis, particularly in prodromal and preclinical phases [2,3]. Decreases of cerebral glucose metabolism in temporo-parietal and precuneus regions as measured by  $^{18}\text{F}$ -FDG-PET, and the amyloid burden, as detected with amyloid-PET, are adopted in the National Institute of Aging-Alzheimer Association (NIA-AA) criteria for both dementia and MCI due to AD pathology [4,5]. According to these criteria,  $^{18}\text{F}$ -FDG-PET hypometabolism and amyloid-PET positivity, reflecting respectively downstream neuronal degeneration and pathological amyloid deposition, are both considered *in vivo* supporting biomarkers for AD pathology and are required to establish diagnosis [4,5]. At difference, the International Working Group criteria (IWG-2) have proposed a simplified algorithm in which only cerebrospinal fluid (CSF) measurements of amyloid and tau protein or amyloid-PET status are considered as supportive diagnostic biomarkers of AD pathology [6], while  $^{18}\text{F}$ -FDG-PET is considered only for disease staging and monitoring of the progression [6]. A recent study on the prognostic value of the NIA-AA [5], IWG-2 and IWG-1 criteria [6,7], however, showed that classification according to the NIA-AA criteria, in which PET pathological and neuronal injury biomarkers are both considered for AD diagnosis, reached the highest prediction accuracy for MCI to ADD conversion in a clinical setting [8].

As for prediction of conversion to AD dementia in MCI subjects, both  $^{18}\text{F}$ -FDG-PET and amyloid-PET techniques have shown high variability in their performances, as recently reported in two Cochrane Reviews [9,10]. As for the former [9], the  $^{18}\text{F}$ -FDG-PET meta-analysis showed high variability in sensitivity and specificity, thus advising against  $^{18}\text{F}$ -FDG-PET routine utilization in MCI subjects [9]. A critical stance by the European Association of Nuclear Medicine (EANM) followed [11]; highlighting the limitations of the Cochrane review and claiming that the observed variability was mostly due to confounding biases, among them, crucially, the methodology to define  $^{18}\text{F}$ -FDG-PET scan positivity [11]. Similarly, the Cochrane review on  $^{11}\text{C}$ -PiB-PET for risk assessment in MCI and differential diagnosis of dementias [10] concluded for a considerable heterogeneity in the conduct and interpretation of the results, particularly due to the lack of defined thresholds for test positivity and standardization of analysis methods, thus not recommending amyloid PET in routine

clinical practice [10]. Other sources of variability for  $^{11}\text{C}$ -PiB-PET results relate crucially to the different follow-up durations employed by different studies, as well as to sampling bias related to varying operational MCI definitions, accordingly to a recent review [12].

Thus, the adoption of validated and standardized methods for  $^{18}\text{F}$ -FDG-PET and amyloid-PET in research and clinical settings is fundamental to achieve high accuracy, as shown in two large recent meta-analyses [13,14]. This is especially true since the role for  $^{18}\text{F}$ -FDG-PET in the early and differential diagnosis of dementias and for amyloid PET in excluding the presence of underlying Alzheimer's disease pathology is confirmed by several reports [15-21].

In a sample of MCI subjects evaluated in a clinical setting, we investigated the separate and combined performances of  $^{18}\text{F}$ -FDG-PET and  $^{11}\text{C}$ -PiB-PET imaging, respectively analyzed with an optimized SPM procedure [22,23] and semi-quantified SUVR methods [24], in predicting or excluding ADD conversion at the individual level. A follow-up period confirmed the ADD conversion or the stable MCI condition.

## **2. Methods**

### *2.1 Participants*

We included 30 MCI subjects, classified according to diagnostic criteria [1], all of them retrospectively included from the database of the Karolinska Institutet, Stockholm, Sweden. Inclusion criteria for the study were the availability of both  $^{11}\text{C}$ -PiB-PET and  $^{18}\text{F}$ -FDG-PET imaging and a clinical follow-up to evaluate the conversion to ADD. MCI clinical subtypes were assessed following standardized criteria [1], thus splitting the whole sample in amnesic/non-amnesic, single- or multiple-domain MCI (aMCI SD, aMCI MD, naMCI SD, naMCI MD, see Table 1). Progression from MCI to ADD was established according to standardized clinical diagnostic criteria [5]. At the clinical follow-up, 14 MCI converted to ADD (median time to conversion 21.5, inter-quartile range IQR 34.8 months) and 16 MCI remained stable (median 31.5 months, IQR 25.8 months). Demographic and clinical summary for the whole cohort and split by conversion status is available in Table 1. All subjects, or their informants/caregivers, gave written informed consent to the experimental procedure that had been approved by the regional Human Ethics Committee of Stockholm as well as the by the radiation safety committee of Uppsala University Hospital.

## 2.2 Cognitive Assessment

Global cognitive functioning at baseline was assessed using Mini Mental Status Examination (MMSE). Multiple cognitive domains were evaluated adopting an extended standardized neuropsychological battery. The neuropsychological tests included the Swedish versions of the Wechsler Adult Intelligence Scale (WAIS), including the Full Scale Intelligence Quotient (FSIQ), Information, Similarities and Block Design subscales. Additionally, verbal short-term memory (Digit Span, Rey Auditory Verbal Learning Test – RAVLT immediate recall), short-term memory, attention and processing speed (Digit Symbol), visuo-constructive abilities (Rey Figure copy), long-term episodic memory (RAVLT delayed recall), long-term visual spatial memory (Rey Figure recall), and visuo-motor, executive and attention functioning (Trail Making Test – A/B) tests. In order to analyze neuropsychological measures, raw scores were transformed into z-scores according to the national normative data [25].

## 2.3 PET Studies

### 2.3.1 $^{18}\text{F}$ -FDG-PET acquisition

$^{18}\text{F}$ -FDG-PET scans were acquired either with a Siemens ECAT EXACT HR+ or a GEMS Discovery ST PET/CT scanner with 3D mode yielding a 155-157 mm axial field of view. The injected dose was  $214 \pm 45$  MBq, and was acquired through a 3D dynamic scan of either 60 (5x60, 5x180, 6x300, 1x600s) or 45 minutes (1x60, 1x1140, 5x300s / 4x30, 9x60, 3x180, 5x300s). Image reconstruction protocol followed a 3D Filtered Back Projection (FBP). Attenuation correction was performed with rotating  $^{68}\text{Ge}$  rod sources for the ECAT EXACT HR+ scanner whereas it was CT-based for the GEMS Discovery-ST. All reconstructed frames were re-aligned to correct for between frame patient motions (VOIager).

### 2.3.2 $^{18}\text{F}$ -FDG-PET data analysis

Image analysis was carried out with SPM5 software (Wellcome Department of Imaging Neuroscience, London, UK; [www.fil.ion.ucl.ac.uk/spm](http://www.fil.ion.ucl.ac.uk/spm)) on MATLAB 8 (MathWorks Inc, Sherborn, Mass). The late 15-min summation image of each  $^{18}\text{F}$ -FDG-PET scan was analyzed according to an optimized  $^{18}\text{F}$ -FDG-PET SPM procedure previously developed and validated in early and differential dementia diagnosis [18,23,26-29] and in prodromal MCI outcome prediction [17]. Briefly, 1. scans were ‘spatially normalized’ in accordance to a reference “dementia specific”  $^{18}\text{F}$ -FDG-PET template [22] and then smoothed 8mm, 2. these single-subject images were compared to a normality database tool by means of a two-sample t-test implemented in SPM5 to

assess brain hypometabolism (detailed description available in [22,23]). The statistical threshold was set at  $p=0.05$ , Family Wise Error (FWE) corrected for multiple comparisons. Only clusters containing more than 100 voxels were deemed to be significant. This method has been shown to be valid, accurate and reliable in detecting AD metabolic signature independently from the PET scanner used for image acquisition [30].

### 2.3.3 $^{11}\text{C}$ -PiB-PET acquisition

Amyloid-PET scans were performed using  $^{11}\text{C}$ -PiB-PET and either a Siemens ECAT EXACT HR+ scanners or a GEMS Discovery ST PET/CT scanner with 3D mode yielding a 155-157 mm axial field of view. The mean injected dose was  $247\pm 72$  MBq. The  $^{11}\text{C}$ -PiB-PET scans consisted of 24 frames (4x30; 9x60; 3x180; 8x300s) with a total duration of 60 minutes with a FBP protocol adopted for image reconstruction. Attenuation correction was performed with rotating  $^{68}\text{Ge}$  rod sources for the ECAT EXACT HR+ scanner whereas it was CT-based for the GEMS Discovery-ST. All reconstructed frames were re-aligned to correct for between frame patient motions (VOIager).

### 2.3.4 $^{11}\text{C}$ -PiB-PET data analysis

$^{11}\text{C}$ -PiB-PET late 40-60 minutes summation images were created and nonlinearly spatially normalised to a population-based PiB template in Montreal Neurological Institute (MNI) space [24] with the use of SPM8 software. A cerebellar grey matter region [24] was used as reference for each 40-60min PiB image to create Standardized Uptake Value ratio ( $\text{SUVR}_{\text{CERGM}}$ ) parametric images.

## 2.4 Neuroimaging biomarkers positivity

### 2.4.1 $^{18}\text{F}$ -FDG-PET

The single-subject  $^{18}\text{F}$ -FDG-PET SPM hypometabolism maps were evaluated by four experts in neuroimaging, blind to each other and to clinical information and amyloid status. The expert raters showed a high agreement (Cohen's  $k$ : 0.89) in the evaluation of SPM maps. Images were defined as AD-positive pattern (FDG+) when  $^{18}\text{F}$ -FDG-PET SPM hypometabolism maps represented either the typical (temporoparietal and/or posterior cingulate hypometabolism) [18,23,31] or an AD atypical pattern as follows: 1. predominant left posterior perisylvian and parietal hypometabolism, suggestive for the logopenic variant of primary progressive aphasia (lvPPA) [32], 2. predominant posterior parietal and occipital brain hypometabolism for posterior cortical atrophy (PCA) [26,33] and 3. frontal and temporo-parietal hypometabolism with posterior cingulate

involvement for the frontal variant AD [34]. Otherwise, the  $^{18}\text{F}$ -FDG-PET SPM hypometabolism maps were defined as AD-negative pattern (FDG-) when they did not show differences in the comparison with normal control database.

#### 2.4.2 $^{11}\text{C}$ -PiB-PET

Composite amyloid SUVR scores resulting from the average of uptake values of medial orbitofrontal, superior parietal, middle temporal, precuneus, anterior and posterior cingulate regions were estimated. We adopted template-based Regions of Interest (ROIs) created through the Wake Forest University PickAtlas toolbox for SPM [35], using anatomical definitions from the Automated Anatomical Labeling (AAL) atlas [36]. These composite SUVR scores were then compared to a validated cut-off threshold, *i.e.* 1.41 [24]. All the subjects were classified as amyloid positive (Amy+) when their composite cortical SUVR score was above the normality cut-off threshold, and as amyloid negative (Amy-), when it was below the normality cut-off threshold.

#### 2.5 Biomarkers analysis for progression prediction

We first evaluated the separate ability of both PET biomarkers in predicting or excluding conversion to dementia, as established at the clinical follow-up diagnosis. We then estimated sensitivity, specificity, accuracy for each PET biomarker, together with a Receiver Operating Characteristic (ROC) analysis with Area Under the Curve (AUC) estimation, which was performed setting clinical status at last follow-up as the primary outcome. Second, to evaluate the combined diagnostic power of both PET biomarkers, we ran a forward conditional logistic regression, setting  $^{18}\text{F}$ -FDG-PET and  $^{11}\text{C}$ -PiB-PET results (FDG+/- and Amy +/-) as predictors and dementia conversion status as outcome. This procedure allows the creation of a third variable in which each subject has a predicted probability value according to the combination of  $^{18}\text{F}$ -FDG-PET and  $^{11}\text{C}$ -PiB-PET ratings. We then used this third variable to test the classification ability of the biomarkers combination in predicting conversion to AD dementia. Considering the group as split by biomarker combination status (e.g. FDG+/Amy+, FDG-/Amy-), we estimated a Kaplan-Meier survival distribution considering ADD conversion as event as a function of the follow-up time. All the statistical analyses were performed with SPSS software (v21.0 <http://www.ibm.com/analytics/us/en/technology/spss/>)

### 3. Results

#### 3.1 Cognitive Assessment

Converter MCI when compared to the non-converters showed more impairment at baseline in the long-term visual spatial memory task (Rey Figure recall) (Mann-Whitney non-parametric U test,  $p=0.011$ ) and in the WAIS Similarities subscale (Mann-Whitney non-parametric U test,  $p=0.011$ ). No significant differences were found in the other neuropsychological test scores at baseline between the two MCI subgroups. A summary of neuropsychological data is available in Table 2.

#### 3.2 Biomarkers positivity

Within the 14 converter MCI cases, 11 were FDG+/Amy+, showing both the typical pattern (N=4) and atypical AD brain glucose hypometabolism patterns (*i.e.*, 2 lvPPA, 2 PCA and 1 frontal variant of AD patterns). In addition, there were 2 subjects with a typical AD hypometabolism pattern with mixed evidence for cerebrovascular disease. Finally, the other 3 MCI converter cases were FDG-/Amy+. All the 16 non-converter MCI cases were FDG-negative. As regards  $^{11}\text{C}$ -PiB-PET, 10/16 were Amy- and 6/16 were Amy+. The results are summarized on Table 3. Figure 1 depicts representative  $^{18}\text{F}$ -FDG-PET for typical AD, lvPPA and PCA patterns with the respective  $^{11}\text{C}$ -PiB SUVRs maps.

#### 3.3 Biomarkers progression prediction

Both modalities showed valuable prediction ability, with  $^{18}\text{F}$ -FDG-PET positivity performing as the best individual predictor for AD conversion, showing an overall higher accuracy than  $^{11}\text{C}$ -PiB-PET (0.90 vs. 0.80, respectively).  $^{18}\text{F}$ -FDG-PET showed higher specificity than  $^{11}\text{C}$ -PiB-PET (1.00 vs. 0.62), but lower sensitivity (0.79 vs. 1.00). Areas under the curve (AUCs) were 0.89 for  $^{18}\text{F}$ -FDG-PET and 0.81 for  $^{11}\text{C}$ -PiB-PET. Adding genetic risk, *i.e.* APOE status, to either the PET-based measurements did not improve the prediction, or exclusion, of conversion to dementia due to AD.

Noteworthy,  $^{18}\text{F}$ -FDG-PET and  $^{11}\text{C}$ -PiB-PET combined showed the highest AUC (0.96) (see Figure 2A). None of the FDG-/Amy- subjects converted to AD, leading to 1.0 probability of non-conversion at about 10 years from MCI diagnosis. On the other hand, all the FDG+/Amy+ converted within about 8 years of follow-up. Lastly, 3 FDG-/Amy+ subjects converted to ADD either very early after initial MCI diagnosis (N=2, converting after 6 and 7 months of follow-up) or about 7.5 years later (N=1, converting after 90 months of follow-up). Kaplan-Meier curves showed a clear difference between the survival probability of the

FDG+/Amy+, FDG-/Amy+ and FDG-/Amy- groups (see Figure 2B). The right censoring pattern differed across the biomarker groups, in particular with lack of censored events for the FDG+/Amy+ group and complete censoring for the FDG-/Amy-. A log-rank (Mantel-Cox) test confirmed the statistically significant difference between the survival distributions of the three groups ( $\text{Chi}^2$ : 12.051,  $p=0.002$ ). The log-rank test was preferred since it focuses on the longer survival times and is more resistant to differences in the right censoring patterns, which are in contrast with the proportional hazard assumption of the Kaplan-Meier test.

#### 4. Discussion

In this study we investigated, in single MCI individuals, the separate and combined performances of  $^{18}\text{F}$ -FDG-PET and  $^{11}\text{C}$ -PiB-PET measures, using validated semi-quantified methods, as biomarkers of neurodegeneration and pathology status able to exclude or predict the risk of conversion to dementia due to AD. From the clinical and neuropsychological standpoint, at baseline, the converter MCI performed significantly worse than the stable subjects in long-term visual spatial memory (Rey Figure recall) and productive/receptive language (WAIS Similarities subscale). These findings are coherent with the known AD-related neuropsychological signature [5].

The prediction analyses showed partly different performances for topographical ( $^{18}\text{F}$ -FDG-PET) and pathological ( $^{11}\text{C}$ -PiB-PET) biomarkers, with higher specificity for  $^{18}\text{F}$ -FDG-PET SPM maps and higher sensitivity for  $^{11}\text{C}$ -PiB-PET SUVRs. In details, the conversion rate of  $^{18}\text{F}$ -FDG-PET-positive subjects was 100%, whereas the conversion rate of PET amyloid-positive subjects was 70%, consistently with previous literature [24,37]. All the subjects positive for both  $^{18}\text{F}$ -FDG-PET and  $^{11}\text{C}$ -PiB-PET ( $N=11$ ) were diagnosed with dementia due to AD pathology during the follow-up period. The combination of these PET biomarkers showed an increase in overall accuracy for ADD conversion prediction in MCI subjects (Figure 2A).

In this series,  $^{18}\text{F}$ -FDG-PET SPM maps were able to detect not only the typical AD hypometabolism signature, but also the hypometabolism patterns suggestive of atypical clinical presentation of AD pathology (i.e., lvPPA, PCA, and frontal variant) [34] (see Figure 1). The optimized  $^{18}\text{F}$ -FDG-PET SPM method here confirmed previous evidence on its effective role in differentiation of atypical clinical phenotypes associated with AD pathology [26,28]. There is a consistent body of evidence regarding the potential of  $^{18}\text{F}$ -FDG-PET in detecting specific hypometabolism patterns across different dementia conditions, e.g. ADD, Dementia with Lewy Bodies (DLB) and Frontotemporal Dementia (FTD) [17,18,23,38]. The previous literature and present results strongly advocate for a crucial role of topographical downstream neurodegeneration markers, such as

$^{18}\text{F}$ -FDG-PET, particularly in MCI conversion prediction and also in early dementia classification, with critical implications in the use of voxel-wise semiquantitative methods.

Additionally, few  $^{18}\text{F}$ -FDG-PET SPM maps were rated as representative of mixed AD plus cerebrovascular disease (CVD) (see Results). Neuroimaging-based biomarkers have increasingly been recognized as of value for clinical practice in the diagnosis of underlying vascular disease [39,40]. Structural Magnetic Resonance Imaging (MRI) techniques are the standard choice when CVD is suspected, revealing specific imaging abnormalities associated with vascular events [41].  $^{18}\text{F}$ -FDG-PET studies in cerebrovascular diseases have revealed typical patterns of focal scattered and patchy hypometabolism in cortical and subcortical regions [39]. Of note,  $^{18}\text{F}$ -FDG-PET measurement could add to MRI the evidence of dysfunctional areas, due to its sensitivity in detecting cortical deafferentation and synaptic dysfunction in normal-appearing tissue [40].

Crucially, all the subjects negative for both  $^{18}\text{F}$ -FDG-PET and  $^{11}\text{C}$ -PiB-PET remained stable over the follow-up time. This finding supports the fundamental value of both biomarkers in excluding neurodegenerative process due to underlying AD pathology in the MCI stage. This high negative AD dementia risk prediction was driven by the high value of the  $^{18}\text{F}$ -FDG-PET negativity to rule out AD-associated neurodegeneration in MCI cases, as previously found and discussed [17]. The high specificity of  $^{18}\text{F}$ -FDG-PET in ADD, DLB and FTD implies that a negative, or normal scan in the presence of the suspicion of dementia makes a diagnosis of a neurodegenerative disease very unlikely. In the context of early diagnosis, the exclusionary role of  $^{18}\text{F}$ -FDG-PET is especially important in younger subjects with a suspicion of neurodegenerative disease [20]. With regards to amyloid-PET, its potential in ruling out AD pathology is well known [42].

Six out of 16 non-converter MCI showed an Amy+ pattern with a negative  $^{18}\text{F}$ -FDG-PET scan, at a median follow-up time of 25 months. We suggest that these FDG-/Amy+ non-converter MCI cases could either be in need of longer follow-ups or, when remaining stable over long time, could be considered as incidental amyloid cases [43]. In addition, as previously stated, the presence of high PET amyloid burden in MCI subjects does not provide a sufficient confidence of progression to AD dementia [43,44]. A known limit of amyloid-PET imaging regards the prevalence of subjects, increasing with age, who do not develop dementia or do not present cognitive alterations in spite of a significant amyloid burden [43]. For these subjects, the topographical  $^{18}\text{F}$ -FDG-PET downstream biomarker fully shows its potential in ruling out ongoing neurodegenerative process *in vivo* [45].  $^{18}\text{F}$ -FDG-PET imaging has been indeed shown to have a valuable exclusionary role, thus really bearing a crucial added prognostic value in MCI [13,14,20]. Three out of 14 converter MCI cases were FDG negative but Amyloid positive, presenting respectively 6, 7 and 90 months of follow-up. This evidence supports

a possible temporal dissociation between the two PET biomarkers, with an earlier positivity of amyloid-PET imaging in some cases, which supports the need of combined adoption of pathological and neurodegenerative biomarkers, when available.

Only few studies evaluated the impact of  $^{18}\text{F}$ -FDG-PET and  $^{11}\text{C}$ -PiB-PET in the same cohort of MCI subjects, although with inconsistent results, especially with regards to  $^{18}\text{F}$ -FDG-PET imaging [46-49]. Overall, these studies showed lower performances of  $^{18}\text{F}$ -FDG-PET in the MCI to ADD conversion prediction, which is likely to be due to variability in follow-up durations and, more importantly, to the heterogeneity in the analysis methodology [46-49]. The  $^{18}\text{F}$ -FDG-PET quantification methods varied from  $^{18}\text{F}$ -FDG-PET SUVR composite scores [46,48], to the use of fully automated analyses [47,49]. The higher sensitivity and specificity of  $^{18}\text{F}$ -FDG-PET found in the present study is likely related to (1) follow-up lengths, (2) the use of an optimized and validated SPM method for the analysis of  $^{18}\text{F}$ -FDG-PET data with expert image interpretation [23] and (3) the study design. As for the latter, in our retrospective study the MCI subjects within the internal database of a clinical research center are representative of a highly selected group, not reflecting the standard consecutive population observed in a memory clinic. Even if the present results are specific to this experimental clinical scenario, the high accuracy of the optimized  $^{18}\text{F}$ -FDG-PET SPM method in this MCI group was comparable to the accuracy level obtained in more heterogeneous cohorts of MCI subjects, in predicting, or excluding, conversion to different dementia syndromes [17,18,23].

## 5. Conclusion

To date, there are no absolute timing algorithms for diagnosis of dementia due to AD providing clear recommendation for the use of  $^{18}\text{F}$ -FDG-PET and amyloid-PET imaging in a clinical setting [9,10].  $^{18}\text{F}$ -FDG-PET as a biomarker of AD- as well as non-AD neurodegeneration has shown a very high specificity, which is of utmost relevance for differential diagnosis in the early phase of dementia and for the exclusion of underlying neurodegenerative processes. On the other hand, amyloid-PET represents a unique biomarker with exceptional sensitivity for *in vivo* investigation of underlying cerebral AD pathology.

There is some added value for the combined use of these PET biomarkers, especially when adopted with validated quantification approaches as shown in the present study, given that the combination of these techniques improved the global accuracy of ADD conversion prediction. We suggest however, that the recommendation for adoption of both PET techniques for MCI prognosis should be tailored on the individual cases, taking into account clinical, neuropsychological and the available of other biomarker data.

Finally, this work contributes to the need for standardization of core biomarkers collection and measurements and the urgency to develop evidence-based guidelines for high-level accuracy biomarkers, useful for early dementia diagnosis, and in particular for the inclusion or exclusion in prevention clinical trials [50].

## **6. Acknowledgments**

L.I. holds a ministerial fellowship granted by the Italian Ministry of Education, University and Research (Graduate program). The research received funding from the Italian Ministry of Health (Ricerca Finalizzata Progetto Reti Nazionali AD NET-2011- 02346784), from the EU FP7 INMIND Project (FP7-HEALTH-2011-two-stage “Imaging of Neuroinflammation in Neurodegenerative Diseases”, grant agreement no. 278850) and from the Joint Program on Neurodegenerative Disorders (EU-JPND) project Biomarkers for Alzheimer's Disease and Parkinson's Diagnostics (BIOMARKAPD).

K.C and A.N. were financially supported by the Swedish Research Council (project 05817), Swedish Brain Power, the Regional Agreement on Medical Training and Clinical Research (ALF) for Stockholm County Council, the Strategic Research Programme in Neuroscience at Karolinska Institutet, the Foundation for Old Servants, Gun and Bertil Stohne's Foundation, KI Foundations, the Swedish Brain Foundation, the Swedish Alzheimer's Foundation (Alzheimerfonden), Demensfonden, the Wenner-Gren Foundation, the European Union's Seventh Framework Programme (FP7/2007-2013) under grant agreement n° HEALTH-F2-2011-278850 (INMiND), and the Swedish Foundation for Strategic Research (SSF).

KC and AN wish to thank Mr. Johan Lilja for support related to the imaging software VOIager. LI, PA, VB and DP wish to thank Dr. Luca Presotto for its assistance in image handling and Dr. Tommaso Ballarini and Dr. Silvia Paola Caminiti for their comments on the work.

**Conflict of Interest:** The authors have no conflict of interest to report.

## 7. References

- [1] Petersen RC, Caracciolo B, Brayne C, Gauthier S, Jelic V, Fratiglioni L (2014) Mild cognitive impairment: a concept in evolution. *J. Intern. Med.* **275**, 214–228.
- [2] Hampel H, Frank R, Broich K, Teipel SJ, Katz RG, Hardy J, Herholz K, Bokde ALW, Jessen F, Hoessler YC, Sanhai WR, Zetterberg H, Woodcock J, Blennow K (2010) Biomarkers for Alzheimer's disease: academic, industry and regulatory perspectives. *Nat Rev Drug Discov* **9**, 560–574.
- [3] Shaw LM, Korecka M, Clark CM, Lee VMY, Trojanowski JQ (2007) Biomarkers of neurodegeneration for diagnosis and monitoring therapeutics. *Nat Rev Drug Discov* **6**, 295–303.
- [4] Albert MS, DeKosky ST, Dickson D, Dubois B, Feldman HH, Fox NC, Gamst A, Holtzman DM, Jagust WJ, Petersen RC, Snyder PJ, Carrillo MC, Thies B, Phelps CH (2011) The diagnosis of mild cognitive impairment due to Alzheimer's disease: Recommendations from the National Institute on Aging-Alzheimer's Association workgroups on diagnostic guidelines for Alzheimer's disease. *Alzheimer's & Dementia* **7**, 270–279.
- [5] McKhann GM, Knopman DS, Chertkow H, Hyman BT, Jack CR Jr., Kawas CH, Klunk WE, Koroshetz WJ, Manly JJ, Mayeux R, Mohs RC, Morris JC, Rossor MN, Scheltens P, Carrillo MC, Thies B, Weintraub S, Phelps CH (2011) The diagnosis of dementia due to Alzheimer's disease: Recommendations from the National Institute on Aging-Alzheimer's Association workgroups on diagnostic guidelines for Alzheimer's disease. *Alzheimer's & Dementia* **7**, 263–269.
- [6] Dubois B, Feldman HH, Jacova C, Hampel H, Molinuevo JL, Blennow K, DeKosky ST, Gauthier S, Selkoe D, Bateman R, Cappa S, Crutch S, Engelborghs S, Frisoni GB, Fox NC, Galasko D, Habert M-O, Jicha GA, Nordberg A, Pasquier F, Rabinovici G, Robert P, Rowe C, Salloway S, Sarazin M, Epelbaum S, de Souza LC, Vellas B, Visser PJ, Schneider L, Stern Y, Scheltens P, Cummings JL (2014) Advancing research diagnostic criteria for Alzheimer's disease: the IWG-2 criteria. *Lancet Neurology* **13**, 614–629.
- [7] Dubois B, Feldman HH, Jacova C, DeKosky ST, Barberger-Gateau P, Cummings J, Delacourte A, Galasko D, Gauthier S, Jicha G (2007) Research criteria for the diagnosis of Alzheimer's disease: revising the NINCDS–ADRDA criteria. *The Lancet Neurology* **6**, 734–746.
- [8] Vos SJB, Verhey F, Frölich L, Kornhuber J, Wiltfang J, Maier W, Peters O, Rütger E, Nobili F, Morbelli S, Frisoni GB, Drzezga A, Didic M, van Berckel BNM, Simmons A, Soininen H,

- Kłoszewska I, Mecocci P, Tsolaki M, Vellas B, Lovestone S, Muscio C, Herukka S-K, Salmon E, Bastin C, Wallin A, Nordlund A, de Mendonça A, Silva D, Santana I, Lemos R, Engelborghs S, Van der Mussele S, Alzheimer's Disease NeuroImaging Initiative, Freund-Levi Y, Wallin ÅK, Hampel H, van der Flier W, Scheltens P, Visser PJ (2015) Prevalence and prognosis of Alzheimer's disease at the mild cognitive impairment stage. *Brain* **138**, 1327–1338.
- [9] Smailagic N, Vacante M, Hyde C, Martin S, Ukoumunne O, Sachpekidis C (2015) <sup>18</sup>F-FDG PET for the early diagnosis of Alzheimer's disease dementia and other dementias in people with mild cognitive impairment (MCI). *Cochrane Database Syst Rev* **1**, CD010632.
- [10] Zhang S, Smailagic N, Hyde C, Noel-Storr AH, Takwoingi Y, McShane R, Feng J (2014) (11)C-PIB-PET for the early diagnosis of Alzheimer's disease dementia and other dementias in people with mild cognitive impairment (MCI). *Cochrane Database Syst Rev* **7**, CD010386.
- [11] Morbelli S, Garibotto V, Van De Giessen E, Arbizu J, Chételat G, Drezgza A, Hesse S, Lammertsma AA, Law I, Papatà S, Payoux P, Pagani M, European Association of Nuclear Medicine (2015) A Cochrane review on brain [(18)F]FDG PET in dementia: limitations and future perspectives. *Eur J Nucl Med Mol Imaging* **42**, 1487–1491.
- [12] Ma Y, Zhang S, Li J, Zheng D-M, Guo Y, Feng J, Ren W-D (2014) Predictive accuracy of amyloid imaging for progression from mild cognitive impairment to Alzheimer disease with different lengths of follow-up: a meta-analysis. [Corrected]. *Medicine (Baltimore)* **93**, e150.
- [13] Frisoni GB, Bocchetta M, Chételat G, Rabinovici GD, de Leon MJ, Kaye J, Reiman EM, Scheltens P, Barkhof F, Black SE (2013) Imaging markers for Alzheimer disease Which vs how. *Neurology* **81**, 487–500.
- [14] Perani D, Schillaci O, Padovani A, Nobili FM, Iaccarino L, Della Rosa PA, Frisoni G, Caltagirone C (2014) A survey of FDG- and amyloid-PET imaging in dementia and GRADE analysis. *Biomed Res Int* **2014**, 785039.
- [15] Rowe CC, Ng S, Ackermann U, Gong SJ, Pike K, Savage G, Cowie TF, Dickinson KL, Maruff P, Darby D, Smith C, Woodward M, Merory J, Tochon-Danguy H, O'Keefe G, Klunk WE, Mathis CA, Price JC, Masters CL, Villemagne VL (2007) Imaging beta-amyloid burden in aging and dementia. *Neurology* **68**, 1718–1725.
- [16] Rabinovici GD, Furst AJ, O'Neil JP, Racine CA, Mormino EC, Baker SL, Chetty S, Patel P, Pagliaro TA, Klunk WE, Mathis CA, Rosen HJ, Miller BL, Jagust WJ (2007) 11C-PIB PET imaging in

- Alzheimer disease and frontotemporal lobar degeneration. *Neurology* **68**, 1205–1212.
- [17] Cerami C, Della Rosa PA, Magnani G, Santangelo R, Marcone A, Cappa SF, Perani D (2015) Brain metabolic maps in Mild Cognitive Impairment predict heterogeneity of progression to dementia. *YNICL* **7**, 187–194.
- [18] Perani D, Cerami C, Caminiti SP, Santangelo R, Coppi E, Ferrari L, Pinto P, Passerini G, Falini A, Iannaccone S, Cappa SF, Comi G, Gianolli L, Magnani G (2016) Cross-validation of biomarkers for the early differential diagnosis and prognosis of dementia in a clinical setting. *Eur J Nucl Med Mol Imaging* **43**, 499–508.
- [19] Rabinovici GD, Rosen HJ, Alkalay A, Kornak J, Furst AJ, Agarwal N, Mormino EC, O'Neil JP, Janabi M, Karydas A, Growdon ME, Jang JY, Huang EJ, DeArmond SJ, Trojanowski JQ, Grinberg LT, Gorno-Tempini ML, Seeley WW, Miller BL, Jagust WJ (2011) Amyloid vs FDG-PET in the differential diagnosis of AD and FTL. *Neurology* **77**, 2034–2042.
- [20] Jagust W, Reed B, Mungas D, Ellis W, DeCarli C (2007) What does fluorodeoxyglucose PET imaging add to a clinical diagnosis of dementia? *Neurology* **69**, 871–877.
- [21] Ng SY, Villemagne VL, Masters CL, Rowe CC (2007) Evaluating atypical dementia syndromes using positron emission tomography with carbon 11 labeled Pittsburgh Compound B. *Arch Neurol* **64**, 1140–1144.
- [22] Della Rosa PA, Cerami C, Gallivanone F, Prestia A, Caroli A, Castiglioni I, Gilardi MC, Frisoni G, Friston K, Ashburner J, Perani D, EADC-PET Consortium (2014) A standardized [18F]-FDG-PET template for spatial normalization in statistical parametric mapping of dementia. *Neuroinformatics* **12**, 575–593.
- [23] Perani D, Della Rosa PA, Cerami C, Gallivanone F, Fallanca F, Vanoli EG, Panzacchi A, Nobili F, Pappatà S, Marcone A, Garibotto V, Castiglioni I, Magnani G, Cappa SF, Gianolli L, EADC-PET Consortium (2014) Validation of an optimized SPM procedure for FDG-PET in dementia diagnosis in a clinical setting. *YNICL* **6**, 445–454.
- [24] Nordberg A, Carter SF, Rinne J, Drzezga A, Brooks DJ, Vandenberghe R, Perani D, Forsberg A, Langstrom B, Scheinin N, Karrasch M, Någren K, Grimmer T, Miederer I, Edison P, Okello A, Van Laere K, Nelissen N, Vandenbulcke M, Garibotto V, Almkvist O, Kalbe E, Hinz R, Herholz K (2013) A European multicentre PET study of fibrillar amyloid in Alzheimer's disease. *Eur J Nucl Med Mol Imaging* **40**, 104–114.

- [25] Bergman I, Blomberg M, Almkvist O (2007) The importance of impaired physical health and age in normal cognitive aging. *Scand J Psychol* **48**, 115–125.
- [26] Cerami C, Crespi C, Della Rosa PA, Dodich A, Marcone A, Magnani G, Coppi E, Falini A, Cappa SF, Perani D (2015) Brain changes within the visuo-spatial attentional network in posterior cortical atrophy. *J. Alzheimers Dis.* **43**, 385–395.
- [27] Cerami C, Dodich A, Lettieri G, Iannaccone S, Magnani G, Marcone A, Gianolli L, Cappa SF, Perani D (2016) Different FDG-PET metabolic patterns at single-subject level in the behavioral variant of fronto-temporal dementia. *CORTEX* **83**, 101–112.
- [28] Cerami C, Dodich A, Greco L, Iannaccone S, Magnani G, Marcone A, Pelagallo E, Santangelo R, Cappa SF, Perani D (2017) The Role of Single-Subject Brain Metabolic Patterns in the Early Differential Diagnosis of Primary Progressive Aphasias and in Prediction of Progression to Dementia. *J. Alzheimers Dis.* **55**, 183–197.
- [29] Iaccarino L, Crespi C, Della Rosa PA, Catricalà E, Guidi L, Marcone A, Tagliavini F, Magnani G, Cappa SF, Perani D (2015) The Semantic Variant of Primary Progressive Aphasia: Clinical and Neuroimaging Evidence in Single Subjects. *PLoS ONE* **10**, e0120197–17.
- [30] Presotto L, Ballarini T, Caminiti SP, Bettinardi V, Gianolli L, Perani D (2017) Validation of (18)F-FDG-PET Single-Subject Optimized SPM Procedure with Different PET Scanners. *Neuroinformatics* 1–13.
- [31] Herholz K, Salmon E, Perani D, Baron J-C, Holthoff V, Frölich L, Schönknecht P, Ito K, Mielke R, Kalbe E, Zündorf G, Delbeuck X, Pelati O, Anchisi D, Fazio F, Kerrouche N, Desgranges B, Eustache F, Beuthien-Baumann B, Menzel C, Schröder J, Kato T, Arahata Y, Henze M, Heiss WD (2002) Discrimination between Alzheimer dementia and controls by automated analysis of multicenter FDG PET. *NeuroImage* **17**, 302–316.
- [32] Gorno-Tempini ML, Hillis AE, Weintraub S, Kertesz A, Mendez M, Cappa SF, Ogar JM, Rohrer JD, Black S, Boeve BF, Manes F, Dronkers NF, Vandenberghe R, Rascovsky K, Patterson K, Miller BL, Knopman DS, Hodges JR, Mesulam MM, Grossman M (2011) Classification of primary progressive aphasia and its variants. *Neurology* **76**, 1006–1014.
- [33] Crutch SJ, Lehmann M, Schott JM, Rabinovici GD, Rossor MN, Fox NC (2012) Posterior cortical atrophy. *Lancet Neurology* **11**, 170–178.
- [34] Warren JD, Fletcher PD, Golden HL (2012) The paradox of syndromic diversity in Alzheimer disease.

*Nature Reviews Neurology* **8**, 451–464.

- [35] Maldjian JA, Laurienti PJ, Kraft RA, Burdette JH (2003) An automated method for neuroanatomic and cytoarchitectonic atlas-based interrogation of fMRI data sets. *NeuroImage* **19**, 1233–1239.
- [36] Tzourio-Mazoyer N, Landeau B, Papathanassiou D, Crivello F, Etard O, Delcroix N, Mazoyer B, Joliot M (2002) Automated anatomical labeling of activations in SPM using a macroscopic anatomical parcellation of the MNI MRI single-subject brain. *NeuroImage* **15**, 273–289.
- [37] Forsberg A, Engler H, Almkvist O, Blomquist G, Hagman G, Wall A, Ringheim A, Langstrom B, Nordberg A (2008) PET imaging of amyloid deposition in patients with mild cognitive impairment. *Neurobiology of Aging* **29**, 1456–1465.
- [38] Kato T, Inui Y, Nakamura A, Ito K (2016) Brain fluorodeoxyglucose (FDG) PET in dementia. *Ageing Research Reviews* **30**, 73–84.
- [39] Heiss W-D, Zimmermann-Meinzingen S (2012) PET imaging in the differential diagnosis of vascular dementia. *Journal of the Neurological Sciences* **322**, 268–273.
- [40] Heiss W-D, Rosenberg GA, Thiel A, Berlot R, de Reuck J (2016) Neuroimaging in vascular cognitive impairment: a state-of-the-art review. *BMC Med* **14**, 174.
- [41] Vitali P, Migliaccio R, Agosta F, Rosen HJ, Geschwind MD (2008) Neuroimaging in dementia. *Semin Neurol* **28**, 467–483.
- [42] Villemagne VL (2016) Amyloid imaging: Past, present and future perspectives. *Ageing Research Reviews* **30**, 95–106.
- [43] Jansen WJ, Ossenkuppele R, Knol DL, Tijms BM, Scheltens P, Verhey FRJ, Visser PJ, Aalten P, Aarsland D, Alcolea D, Alexander M, Almdahl IS, Arnold SE, Baldeiras I, Barthel H, van Berckel BNM, Bibeau K, Blennow K, Brooks DJ, van Buchem MA, Camus V, Cavedo E, Chen K, Chételat G, Cohen AD, Drzezga A, Engelborghs S, Fagan AM, Fladby T, Fleisher AS, van der Flier WM, Ford L, Förster S, Fortea J, Foscett N, Frederiksen KS, Freund-Levi Y, Frisoni GB, Froelich L, Gabryelewicz T, Gill KD, Gkatzima O, Gómez-Tortosa E, Gordon MF, Grimmer T, Hampel H, Hausner L, Hellwig S, Herukka S-K, Hildebrandt H, Ishihara L, Ivanoiu A, Jagust WJ, Johannsen P, Kandimalla R, Kapaki E, Klimkowicz-Mrowiec A, Klunk WE, Köhler S, Koglin N, Kornhuber J, Kramberger MG, Van Laere K, Landau SM, Lee DY, de Leon M, Lisetti V, Lleó A, Madsen K, Maier W, Marcusson J, Mattsson N, de Mendonça A, Meulenbroek O, Meyer PT, Mintun MA, Mok V, Molinuevo JL, Møllergård HM, Morris JC, Mroczko B, Van der Mussele S, Na DL, Newberg A,

- Nordberg A, Nordlund A, Novak GP, Paraskevas GP, Parnetti L, Perera G, Peters O, Popp J, Prabhakar S, Rabinovici GD, Ramakers IHGB, Rami L, Resende de Oliveira C, Rinne JO, Rodrigue KM, Rodríguez-Rodríguez E, Roe CM, Rot U, Rowe CC, Rütther E, Sabri O, Sánchez-Juan P, Santana I, Sarazin M, Schröder J, Schütte C, Seo SW, Soetewey F, Soinen H, Spiru L, Struyfs H, Teunissen CE, Tsolaki M, Vandenberghe R, Verbeek MM, Villemagne VL, Vos SJB, van Waalwijk van Doorn LJC, Waldemar G, Wallin A, Wallin ÅK, Wiltfang J, Wolk DA, Zboch M, Zetterberg H (2015) Prevalence of Cerebral Amyloid Pathology in Persons Without Dementia. *JAMA* **313**, 1924–15.
- [44] Herrup K (2015) The case for rejecting the amyloid cascade hypothesis. *Nat Neurosci* **18**, 794–799.
- [45] Perani D (2014) FDG-PET and amyloid-PET imaging. *Current Opinion in Neurology* **27**, 405–413.
- [46] Brück A, Virta JR, Koivunen J, Koikkalainen J, Scheinin NM, Helenius H, Någren K, Helin S, Parkkola R, Viitanen M, Rinne JO (2013) [11C]PIB, [18F]FDG and MR imaging in patients with mild cognitive impairment. *Eur J Nucl Med Mol Imaging* **40**, 1567–1572.
- [47] Trzepacz PT, Yu P, Sun J, Schuh K, Case M, Witte MM, Hochstetler H, Hake A, Initiative1 ADN (2014) Comparison of neuroimaging modalities for the prediction of conversion from mild cognitive impairment to Alzheimer's dementia. *NBA* **35**, 143–151.
- [48] Hatashita S, Yamasaki H (2013) Diagnosed Mild Cognitive Impairment Due to Alzheimer's Disease with PET Biomarkers of Beta Amyloid and Neuronal Dysfunction. *PLoS ONE* **8**, e66877.
- [49] Grimmer T, Wutz C, Alexopoulos P, Drzezga A, Förster S, Förstl H, Goldhardt O, Ortner M, Sorg C, Kurz A (2016) Visual Versus Fully Automated Analyses of 18F-FDG and Amyloid PET for Prediction of Dementia Due to Alzheimer Disease in Mild Cognitive Impairment. *J. Nucl. Med.* **57**, 204–207.
- [50] Sperling R, Mormino E, Johnson K (2014) The evolution of preclinical Alzheimer's disease: implications for prevention trials. *Neuron* **84**, 608–622.

**Table 1. Demographic and Clinical Summary of the MCI cohort**

Index	Whole Sample (N=30)	Converter MCI cases (N=14)	Non-converter MCI cases (N=16)	p-value
Gender (N Females)	20	10	10	0.709
APOE e4 carriers pos/neg	20/10	12/2	8/8	0.058
Age in years (mean±sd)	63.57±7.78	60.93±7.39	65.87±7.59	0.052
Education in years (mean±sd)	13.03±3.18	13.08±3.52	13.00±2.99	0.714
MMSE at baseline (mean±sd)	27.63±1.56	27.14±1.51	28.06±1.53	0.110
Follow-up in months (median/IQR)	26.5/30	21.5/34.8	31.5/25.8	0.313
<b>Clinical Presentation (N and %)</b>				
aMCI SD	18 (60%)	7 (50%)	11 (68.8%)	0.429
aMCI MD	6 (20%)	3 (21.4%)	3 (18.7%)	
naMCI SD	4 (13.3%)	2 (14.3%)	2 (12.5%)	
naMCI MD	2 (6.7%)	2 (14.3%)	0 (0%)	

Table showing demographic and clinical data of the studied MCI cohort, split by conversion status.

P-values represent the significance of pairwise converter vs. non-converter MCI group comparisons. Fisher Exact Test (two-tailed) was adopted for the bimodal discrete variables, otherwise a two-tailed Chi<sup>2</sup> test was performed.

\* Indicates a significant difference (Mann-Whitney U-test for independent samples)

*Legend: APOE: Apolipoprotein E, MMSE: MiniMental State Examination, IQR: interquartile range, aMCI SD: amnesic MCI single-domain, aMCI MD: amnesic MCI multi-domain, naMCI SD: non-amnesic MCI single-domain, naMCI MD: non-amnesic MCI multi-domain*

**Table 2. Neuropsychological Summary of the MCI cohort**

Test (mean±sd)	Whole Sample (N=30)	Converter MCI cases (N=14)	Non-converter MCI cases (N=16)	p-value
MMSE	27.63±1.56	27.14±1.51	28.06±1.53	0.110
WAIS - FSIQ	-0.85±1.27	-1.42±1.32	-0.42±1.09	0.054
WAIS - Information	-0.36±0.96	-0.63±0.91	-0.14±0.98	0.183
WAIS - Similarities	-0.07±1.22	-0.75±1.33	0.44±0.87	0.011*
WAIS - Block Design	-1.04±1.21	-1.43±1.45	-0.75±0.94	0.174
Rey Figure Copy	-0.99±2.25	-1.77±3.15	-0.35±0.76	0.398
Digit Span	-0.23±1.04	-0.01±0.98	-0.43±1.07	0.400
Corsi Span	-1.14±1.27	-1.15±0.96	-1.13±1.57	0.684
RAVLT immediate	-0.95±1.02	-1.23±1.09	-0.73±0.94	0.324
RAVLT delayed	-1.17±1.12	-1.37±0.88	-1.02±1.28	0.450
Rey Figure Recall	-1.16±0.96	-1.71±0.98	-0.75±0.74	0.011*
Digit Symbol	-0.60±1.29	-1.03±1.51	-0.28±1.03	0.259
Trail Making Test – A	-0.95±1.66	-1.52±2.00	-0.50±1.20	0.167
Trail Making Test – B	-1.25±2.32	-1.89±3.11	-0.73±1.32	0.427

Table showing neuropsychological summary of the studied MCI cohort, split by conversion status.

Values are shown as z-scores, with reported mean±sd.

P-values represent the significance of pairwise converter vs. non-converter MCI group comparisons.

\* Indicates a significant ( $p < 0.05$ ) difference (Mann-Whitney U-test for independent samples)

*Legend: MMSE: MiniMental State Examination, WAIS: Wechsler Adult Intelligence Scale, FSIQ: Full Scale Intelligence Quotient, RAVLT: Rey Auditory Verbal Learning Test. See Methods for details.*

**Table 3. PET Biomarker combinations and conversion to AD dementia**

	<b>Whole Sample (N=30)</b>	<b>Converter MCI cases (N=14)</b>	<b>Non-converter MCI cases (N=16)</b>
<b>FDG+/Amy+ (%N)</b>	11 (37%)	11 (79%)	0 (0%)
<b>FDG-/Amy+ (%N)</b>	9 (30%)	3 (21%)	6 (37%)
<b>FDG-/Amy- (%N)</b>	10 (33%)	0 (0%)	10 (63%)

Table showing combinations of biomarkers positivity and AD conversion in our MCI cohort. Group sizes are also shown.

*Legend: FDG+ = FDG pattern suggestive for AD; FDG- = FDG pattern negative for AD; Amy+ = Amyloid composite <sup>11</sup>C-PiB-PET SUVR above positivity cut-off; Amy- = Amyloid composite <sup>11</sup>C-PiB-PET SUVR below positivity cut-off.*

**Figure Captions:**

**Figure 1:** Optimized  $^{18}\text{F}$ -FDG-PET SPM maps and  $^{11}\text{C}$ -PiB-PET SUVRs in representative MCI cases

Figure showing optimized  $^{18}\text{F}$ -FDG-PET SPM maps and  $^{11}\text{C}$ -PiB-PET  $\text{SUVR}_{\text{CERGM}}$  images of representative MCI cohort split by clinical outcome and biomarkers positivity combinations. Diverging  $^{18}\text{F}$ -FDG-PET hypometabolism SPM patterns representative of the AD variants are associated with comparable  $^{11}\text{C}$ -PiB-PET amyloid retention distributions.

Optimized  $^{18}\text{F}$ -FDG-PET SPM and  $^{11}\text{C}$ -PiB-PET  $\text{SUVR}_{\text{CERGM}}$  images are overlaid on a T1 standard anatomical template with MRICron software (<http://www.mccauslandcenter.sc.edu/crnl/tools>).

**Figure 2:** ROC and Kaplan-Meier curves for ADD conversion prediction

Figure showing ROC and Kaplan-Meier Survival Curves for ADD conversion prediction. (A) ROC curves for the individual  $^{18}\text{F}$ -FDG-PET (violet) and  $^{11}\text{C}$ -PiB-PET (blue) biomarkers, together with their combination (orange). The dashed black line represents a diagonal reference. AUCs were: 0.89 for  $^{18}\text{F}$ -FDG-PET, 0.81 for  $^{11}\text{C}$ -PiB-PET and 0.96 for their combination. (B) Image showing Kaplan-Meier survival plots split by subgroups derived from PET biomarkers positivity combinations, respectively FDG-/Amy- (green), FDG-/Amy+ (red) and FDG+/Amy+ (blue). Dashes represent right censored cases. See text for details.

**Figure 1:** Optimized  $^{18}\text{F}$ -FDG-PET SPM maps and  $^{11}\text{C}$ -PiB-PET SUVRs in representative MCI cases

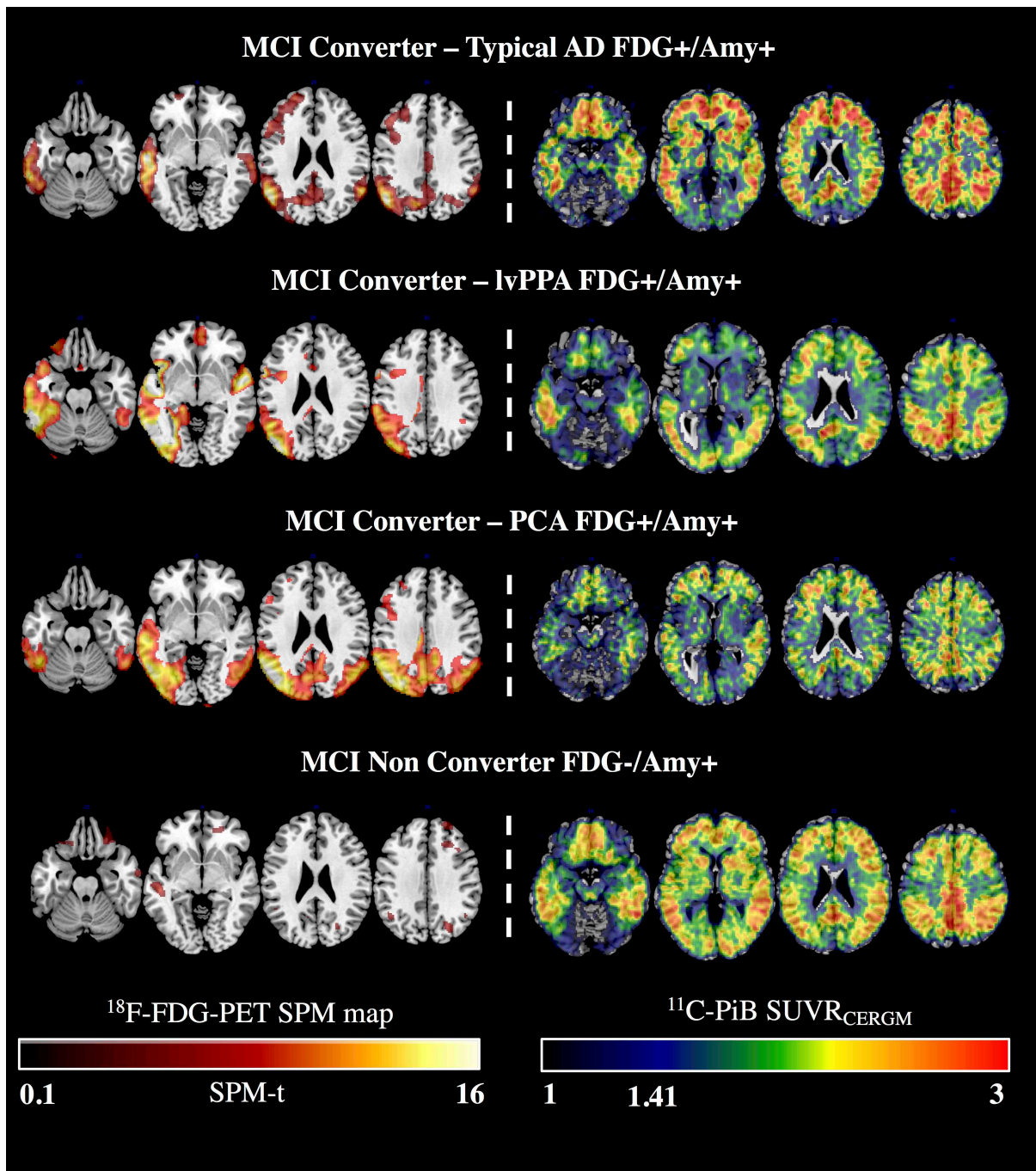


**Figure 2:** ROC and Kaplan-Meier curves for ADD conversion prediction

